Fully Automated Quantification of Left and Right Ventricular Volumes Throughout the Cardiac Cycle from Magnetic Resonance Imaging

Dario Turco, Cristiana Corsi, Claudio Lamberti

DEIS, University of Bologna, Bologna, Italy

Abstract

The left ventricle (LV) has been widely studied and many segmentation methods have been proposed allowing accurate volume estimation from cardiac magnetic resonance imaging (CMRI). Anatomical complexity of the right ventricle (RV) has made accurate determination of RV shape and volume difficult. We propose a fully automated method for both RV and LV segmentation from CMRI. Datasets were analysed using custom software based on a region-based level set model followed by a regularization motion, allowing dynamic endocardial contour detection. RV and LV contours were also manually traced at end-diastole (ED) and end-systole (ES). For both techniques, disk-area summation method was applied to compute volumes. Volumes at ED and ES and ejection fraction were compared. The results of this initial study provide the basis for automated, fast and accurate quantification of LV and RV size, function and volume change throughout the cardiac cycle.

1. Introduction

Quantitative information about ventricle volumes, function and mass is important both in clinical practice and for research purposes. It is well known that for the diagnosis and management of ischaemic and valvular heart disease and cardiomyopathies, the assessment of left ventricular (LV) function is essential, while quantification of LV mass has important prognostic implications [1]. Assessing right ventricular (RV) morphology and function is of paramount importance in the prognosis of patients with pulmonary hypertension, myocardial infarction involving the RV, and LV dysfunction [2,3]. In addition, RV performances define the prognosis in patients with congenital heart disease due to RV volume or pressure overload [4].

Clinicians require measures that are widely available, easily obtained, highly reproducible, and provide clear information on prognosis of heart diseases, likely response to therapy or provide feedback on the success of therapeutic interventions.

Cardiac magnetic resonance imaging is currently the technique of choice for precise measurements of ventricular volumes, function and LV mass. The technique is 3D and hence independent of geometrical assumptions; this, along with its excellent definition of endocardial and epicardial borders, makes it highly accurate and reproducible [5]. These characteristics make temporal follow-up of any individual patient in the clinical setting a realistic possibility.

Currently, manual tracing of endocardial LV and RV boundaries by an expert reader is the standard clinical practice in CMRI. However, this task is labor-intensive and subject to inter- and intra-observer variability. Many algorithms have been introduced to reduce observer variation and improve time efficiency for LV segmentation [6]. Asymmetry and anatomical complexity of the RV has made accurate determination of RV shape and volume difficult and only few studies are reported in literature [7,8].

To overcome these limitations we developed a fast and fully automated method for both RV and LV dynamic segmentation from CMRI.

2. Methods

2.1. CMR imaging and population

CMR data were obtained in 5 patients (3 males; age 37 ± 22 yrs) using a 1.5 Tesla scanner (General Electric) with a phased-array cardiac coil. ECG-gated localizing spin-echo sequences were used to identify the long-axis of the left ventricle. Steady-state free precession dynamic gradient-echo mode (FIESTA) was then used to acquire images during 10 to 15 sec breath-holds. Cine-loops were obtained in 6 to 10 short-axis slices, from the atrio-ventricular ring to the apex (8 mm slice thickness, no gaps) with a temporal resolution of 30 frames per cardiac cycle.

2.2. Image analysis

The first step of the image analysis procedure is the automatic detection of the position of the heart chambers
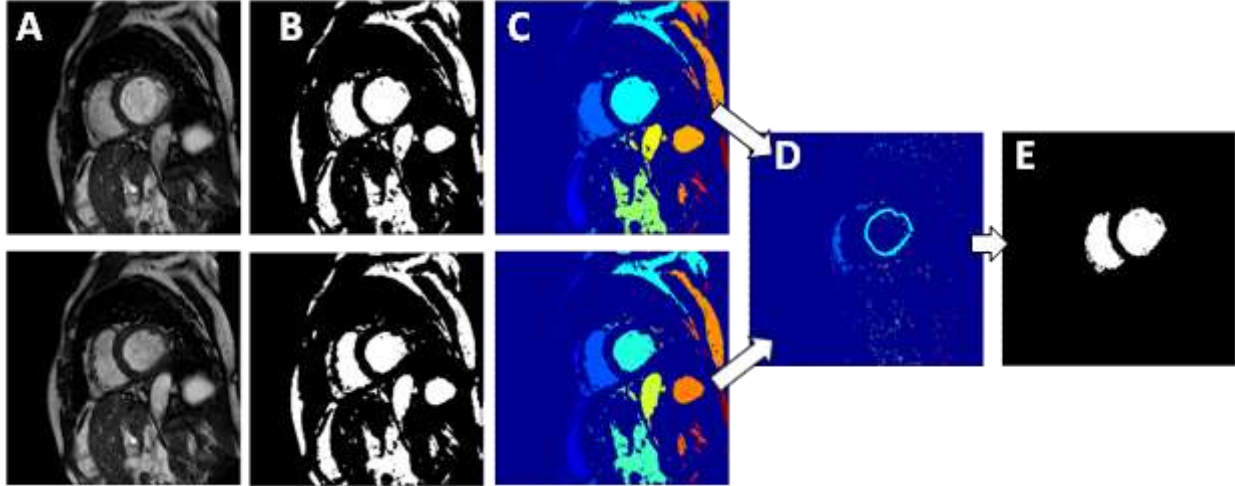
Figure 1. Procedure steps for heart chambers automatic localization (see text for details).

in the 3D data. LV and RV position was automatically detected by studying pixel intensity variations throughout the cardiac cycle.

On the first volume of the acquired sequence corresponding to the ED frame, and on the fifteenth one, the central short-axis slices are selected (figure 1A). A histogram shape-based image thresholding is applied (figure 1B) [9] and the binary images are then labeled (figure 1C). The difference between them (figure 1D) is used to locate the left and right ventricles (figure 1E). Then, we apply morphological operators to dilate and grow this binary image and obtain a mask we will apply to the initial data. Consequently, for each anatomical slice at different height we have a different mask.

An active contour model based on Mumford–Shah segmentation techniques and the level set method is then applied to detect endocardial contours of LV and RV [10]. The model is not based on an edge-function to stop the evolving curve on the desired boundary and can detect objects whose boundaries are not necessarily defined by gradient or with very smooth boundaries, for which the classical active contour models are not applicable. The method considers the evolution of a curve C in order to minimize the energy functional:

$$F(C, c_1, c_2) = \mu \cdot \text{lenght}(C) + \upsilon \cdot \text{area}(\text{inside}(C))$$
$$+ \lambda_1 \int_{\text{inside}(C)} |I(x,y) - c_1|^2 + \lambda_2 \int_{\text{outside}(C)} |I(x,y) - c_2|^2$$

where $I:\Omega c R2 \to R$ is the image, C is an initial curve partitioning the image I, c1 and c2 are the averages of I, respectively, inside and outside C, and $\mu \geq 0$, $\upsilon \geq 0$, $\lambda 1$, $\lambda 2$ are fixed parameters.

The associated level set flow is computed by considering the curve C represented by the zero level set of an implicit function $\varphi:\Omega \to R$ such that $C = \{(x,y)\epsilon\Omega : \varphi(x,y) = 0\}$ and keeping C1 and C2 fixed as:

$$\begin{cases} \partial_t \varphi = \delta(\varphi)\left[\mu \text{div}\left(\frac{\nabla\varphi}{|\nabla\varphi|}\right) - \upsilon - \lambda_1(I - c_1)^2 + \lambda_2(I - c_2)^2 \right] \\ \qquad\qquad\qquad\qquad\qquad\qquad\quad \text{in } \Omega \times]0,\infty[\\ \varphi(0, x, y) = \varphi_0(x, y) \qquad\qquad \text{in } \Omega \\ \\ \frac{\delta(\varphi)\partial\varphi}{|\nabla\varphi|\partial n} = 0 \qquad\qquad\qquad \text{on } \partial\Omega \end{cases}$$

where $\delta()$ is the Dirac function and n denotes the exterior normal to the boundary $\partial \Omega$. The numerical approximation of the model we implemented is described in [10].

The result of this region-based segmentation is then refined applying a regularization motion.

The segmentation procedure is applied to the original images in the region of interest obtained with the application of each specific mask. An example of the final LV and RV segmentation in one central slice at ED is shown in figure 2.

LV slices were manually selected for analysis analysis beginning with the highest basal slice where the LV
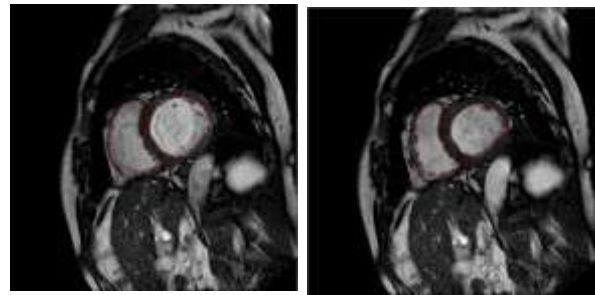

Figure 2. Final LV and RV segmentation in one central slice at ED and ES.

outflow tract was not visible, and ending with the lowest apical slice where the LV cavity was visualized.

RV slices were selected for analysis beginning with the first slice where a pulmonary cusp could be identified (the area of the pulmonary cusp was excluded from the volumes) and ending with the last apical slice to contain blood volume.

In every slice, LV and RV endocardial contours were manually traced frame-by-frame (MASS Analysis, GE) with the papillary muscles included in the ventricular cavities, by an experienced investigator. This resulted in LV and RV cross-sectional area for each slice over time. For both manual and automated techniques, global LV and RV volumes were computed throughout the cardiac cycle using a disk-area summation method, from which end-diastolic and end-systolic volumes (EDV and ESV, respectively) were obtained as the maximum and minimum volumes and LV EF was calculated as (EDV-ESV)/EDV •100.

2.3. Statistical analysis

Statistical analyses were performed using Matlab software (The MathWorks Inc.). Comparisons between automated and manual measurements of EDV, ESV and EF included linear regression and Bland-Altman analyses. The significance of differences between the two techniques was tested using paired t-test. P-values <0.05 were considered significant. In addition, percent discordance between LV volumes obtained by manual tracing and the automated analysis was calculated for each pair of volume curves as the point-by-point sum of absolute differences between the corresponding values, normalized by the point-by-point sum of the manually traced volumes..

3. Results

The automated analysis of a set of images was completed in less than 5 min per patient on a standard personal computer. In contrast, manual tracing of the same images using the standard methodology required between 10 and 20 minutes for each patient.

Figure 3 shows an example of the LV and RV endocardial contours detected at one phase of the cardiac cycle at different levels from LV apex to base. Importantly, papillary muscles and trabeculae were automatically included in the blood pool. Volume-time curves obtained in one patient by manual tracing and by the automated technique are shown in Figure 4.

Linear regression analysis between the automated technique and the manual reference volume values at ED and ES resulted in very good correlation coefficients and regression slopes of for both LV and RV volumes (LV: r=0.99, y=0.98x+2; RV: r=0.99, y=0.87x+15).
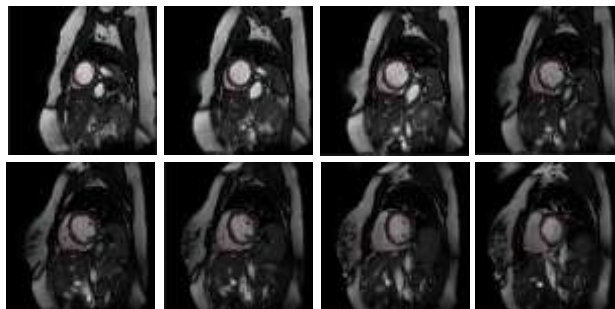

Figure 3. Examle of the detected LV and RV endocardial contours in one frame, from the apex (upper left) to the base (bottom right).
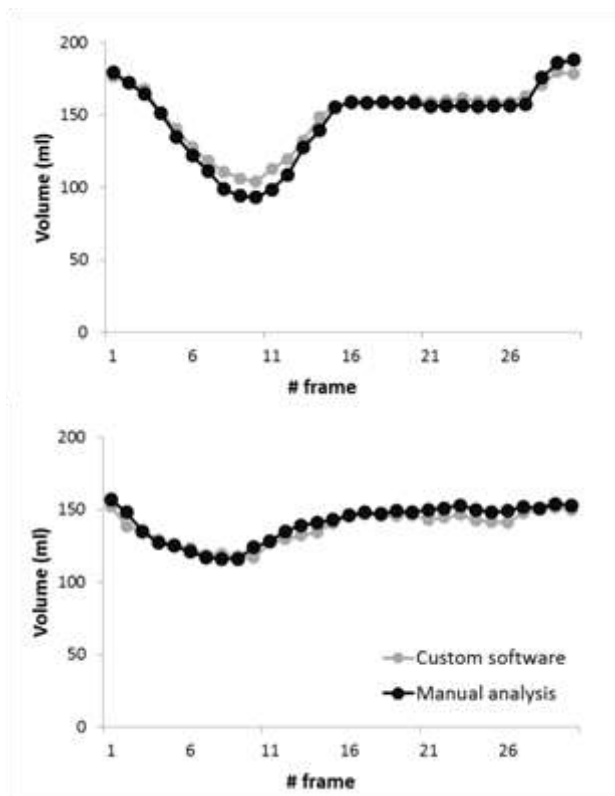

Figure 4. Example of LV (top panel) and RV (bottom panel) volume time curves obtained in one patient, by manual tracing and custom software

High correlation and regression slope were also obtained for LV EF (r=0.98, y=0.95x+0.004).

Bland-Altman analysis showed no significant biases between the automated measurements and the manual reference technique for LV and RV volumes and EF (bias: -0.2ml; -0.8ml; -2%). These biases reflected systematic errors of -0.1%, -0.6% and -6% of the corresponding mean values. The 95% limits of agreement were relatively narrow (LV: 12ml; RV: 17ml; EF: 5.5%), providing additional support to the tight agreement between the two techniques. The calculated percent discordance was only 3.7±0.7% for LV volume-time curves and 3.2±1.4% for RV volume-time curves.

4. Discussion and conclusion

CMR imaging has become the technique of choice for precise measurements of ventricular volumes and function. This imaging technique has excellent definition of endocardial borders and it is highly reproducible [11,12]. In addition, the acquisition time of CMRI scan using the most recent techniques can be as short as 3 min with a high temporal resolution allowing assessment of systolic and diastolic function.

In clinical practice, the analysis of LV volumes is performed by manually tracing LV endocardial contours frame-by-frame on each slice and by the application of geometric modeling in about 15 min per data set. RV analysis is more problematic because it has a complex anatomical shape and is very trabeculated.

New, efficient and robust algorithms need to be developed and tested for automated frame-by-frame LV and RV endocardial contour detection from dynamic CMR images to become feasible in the majority of patients.

In this paper, we propose a segmentation technique based on the minimization of an energy function containing information regarding the grey level values of the pixels into the image. The minimization of this energy function leads to the segmentation of the image in regions for which the difference in the grey level intensity average inside and outside is maximized. Applying this model, we detect objects with boundaries that are either not necessarily defined by a gradient or are very smooth, thus rendering the classical active contour models useless. In addition, the method has no need for a priori knowledge of the shape of the objects to be detected. Importantly, no parameters need to be set in the model and the segmentation of both chambers is fully automated.

The results of this initial study showed that the proposed technique allows fast, automated detection of LV and RV boundaries. The proposed approach is considerably faster than manual tracing and fully automated.

In this initial feasibility study, this technique was found accurate compared to the standard reference methodology but further testing in larger groups of patients is necessary. If verified by further validation studies, this analysis holds promise for multiple clinical applications, such as quantitative assessment of RV performance in congenital heart disease, arrhythmogenic right ventricular cardiomyopathy and primary pulmonary hypertension, evaluation of systolic and diastolic function of both ventricles in a variety of disease states affecting myocardial properties and conduction delays, and extensive monitoring of the impact of therapies.

References

[1] Schillaci G, Verdecchia P, Porcellati C, Cuccurullo O, Cosco C, Perticone F. Continuous relation between left ventricular mass and cardiovascular risk in essential hypertension. Hypertension 2000;35:580–586.

[2] Juilliere Y, Barbier G, Feldmann L, Grentzinger A, Danchin N, Cherrier F. Additional predictive value of both left and right ventricular ejection fractions on long-term survival in idiopathic dilated cardiomyopathy. Eur Heart J 1997; 18:276–80.

[3] Chin KM, Kim NH, Rubin LJ. The right ventricle in pulmonary hypertension. Coron Artery Dis 2005;16:13–8.

[4] Davlouros PA, Niwa K, Webb G, Gatzoulis MA. The right ventricle in congenital heart disease. Heart 2006;92:i27–i38.

[5] Bailly A, Lipiecki J, Chabrot P, Alfidja A. Garcier JM, Ughetto S, Ponsonnaille J, Boyer L. Assessment of left ventricular volumes and function by cine-MR imaging depending on the investigator's experience. Surgical and Radiologic Anatomy 2009;31:113-120.

[6] Lee HY, Codella NCF, Cham MD, Weinsaft JW, Wang Y. Automatic Left Ventricle Segmentation Using Iterative Thresholding and an Active Contour Model With Adaptation on Short-Axis Cardiac MRI. IEEE Trans on Biomed Eng 2010; 57(4):905-913.

[7] Coghlan JG, Davar J. How should we assess right ventricular function in 2008? European Heart Journal Supplements 2007; 9:H22–H28.

[8] Mertens LL, Friedberg MK. Imaging the right ventricle--current state of the art. Nat Rev Cardiol 2010;10:551-63.

[9] Otsu N. A threshold selection method from gray-level histograms. IEEE Trans Sys Man Cyber. 1979;9(1): 62–66.

[10] Chan TF, Vese LA. Active Contours Without Edges. IEEE Trans Image Process 2001;10(2):266-277.

[11] Grothues F, Smith GC, Moon JC, Bellenger NG, Collins P, Klein HU, Pennell DJ. Comparison of interstudy reproducibility of cardiovascular magnetic resonance with twodimensional echocardiography in normal subjects and in patients with heart failure or left ventricular hypertrophy. Am J Cardiol 2002;90:29–34.

[12] Pattynama PM, Lamb HJ, Van der Velde EA, Van der Geest RJ, De Roos A. Reproducibility of MRI-derived measurements of right ventricular volumes and myocardial mass. Magn Reson Imaging 1995;13:53–63.

Address for correspondence.

Cristiana Corsi, PhD
University of Bologna
Viale Risorgimento 2, 40136 Bologna, Italy
E-mail: cristiana.corsi3@unibo.it